Surname *et al. Energy Mater* Year;Volume:Number
DOI: 10.20517/energymater.2021.xx

Energy Materials

Supplementary Material

Rational design of nitrogen-doping $Ti_3C_2T_x$ microspheres with enhanced polysulfide catalytic activity for lithium-sulfur batteries

Lucheng Cai[#], Hangjun Ying[#], Chaowei He, Hui Tan, Pengfei Huang, Qizhen Han, Wei-Qiang Han*

School of Materials Science and Engineering, Zhejiang University, Hangzhou 310058, Zhejiang, China.

[#]Authors contributed equally.

***Correspondence to:** Prof./Dr. Wei-Qiang Han, School of Materials Science and Engineering, Zhejiang University, 866 Yuhangtang Rd, Hangzhou 310058, Zhejiang, China. E-mail: hanwq@zju.edu.cn

ORCID: Wei-Qiang Han(0000-0001-5525-8277)

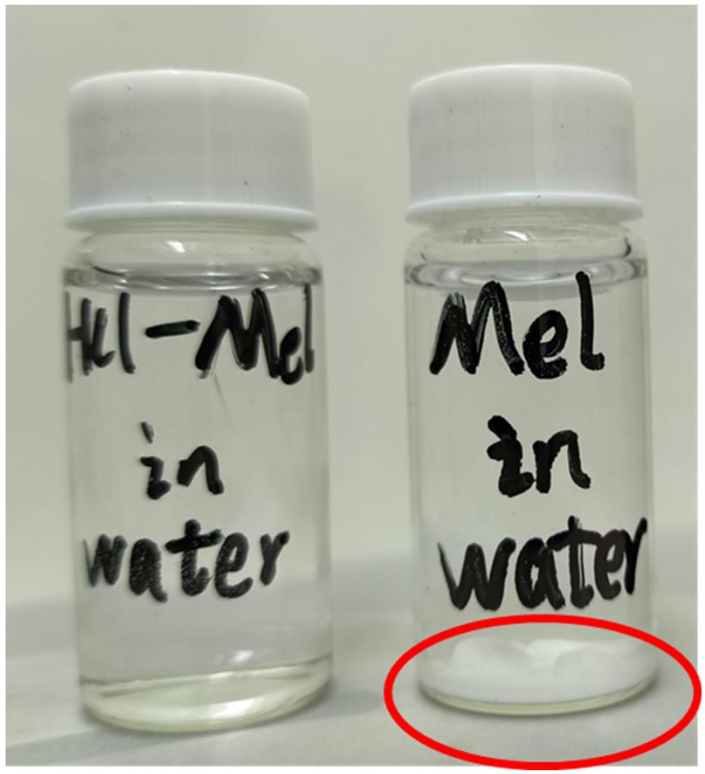

Supplementary Figure 1. A digital photograph showing the treatment of melamine by HCl to make it dissolve in water. Left: HCl- melamine. Right: melamine.

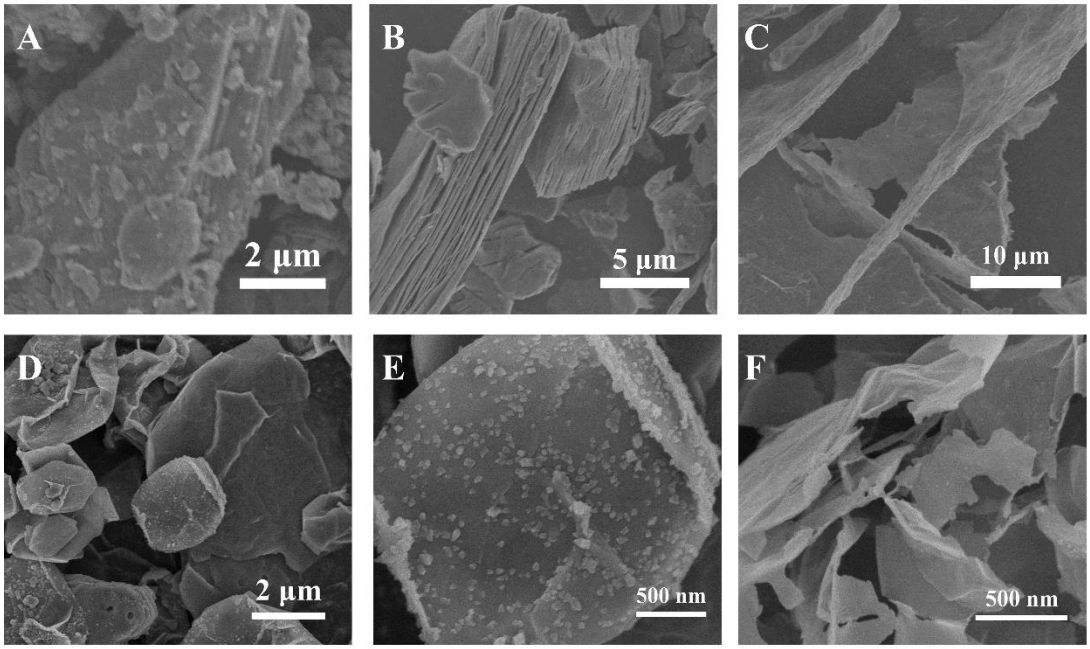

Supplementary Figure 2. SEM images of (A) Ti_3AlC_2, (B) multi-layered $Ti_3C_2T_x$, (C) few-layered $Ti_3C_2T_x$ nanosheets, (D, E) 3D $Ti_3C_2T_x$ and (F) 3D N-$Ti_3C_2T_x$.

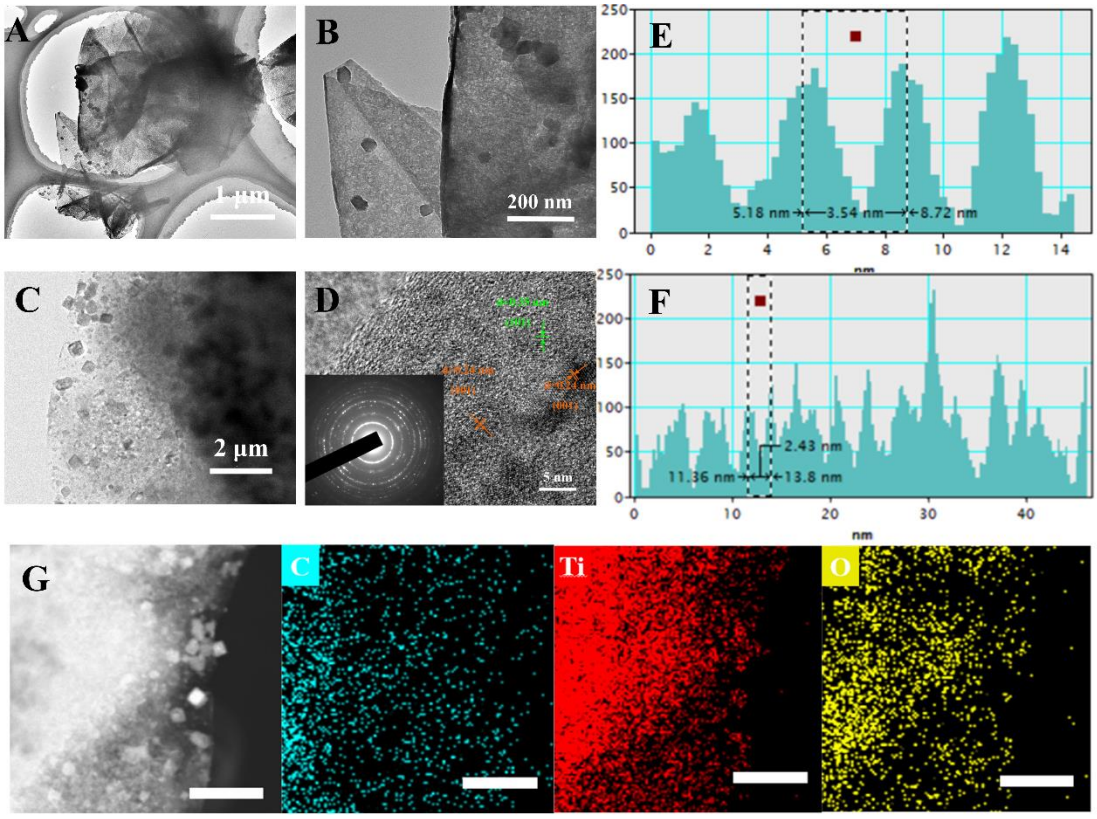

Supplementary Figure 3. (A-C) TEM and (D) HRTEM images of 3D $Ti_3C_2T_x$ (inset: the selected area electron diffraction pattern) and (E-F) corresponding crystal-plane spacing diagram. (G) STEM image of 3D $Ti_3C_2T_x$ and the corresponding elemental mappings of C, Ti, and O. Scale bars: 500 nm (G).

The 3D $Ti_3C_2T_x$ exhibits a wasting-paper morphology composed of MXenes nanosheets, with nanoparticles distributed on the surfaces (**Supplementary Figure 3A** and **B**). The TEM reveals a clear view of these nanoparticles. The HRTEM image of the sample shows distinct lattice stripes, indicating a high degree of crystallization. It also reveals numerous regions with a lattice spacing of approximately 0.24 nm, corresponding to the (0 0 1) crystal plane of TiO_2, as well as a few regions with a lattice spacing of 0.35 nm, corresponding to the (1 0 1) crystal plane of TiO_2. The elemental distribution map demonstrates the presence of C, Ti, and O elements in 3D $Ti_3C_2T_x$. The C element is uniformly distributed, while the distribution of Ti and O elements corresponds to the nanoparticles observed in the STEM image. Due to the high exposure of Ti atoms on the MXenes surface, it exhibits poor thermodynamic stability and spontaneously converts to TiO_2, even in an inert atmosphere.

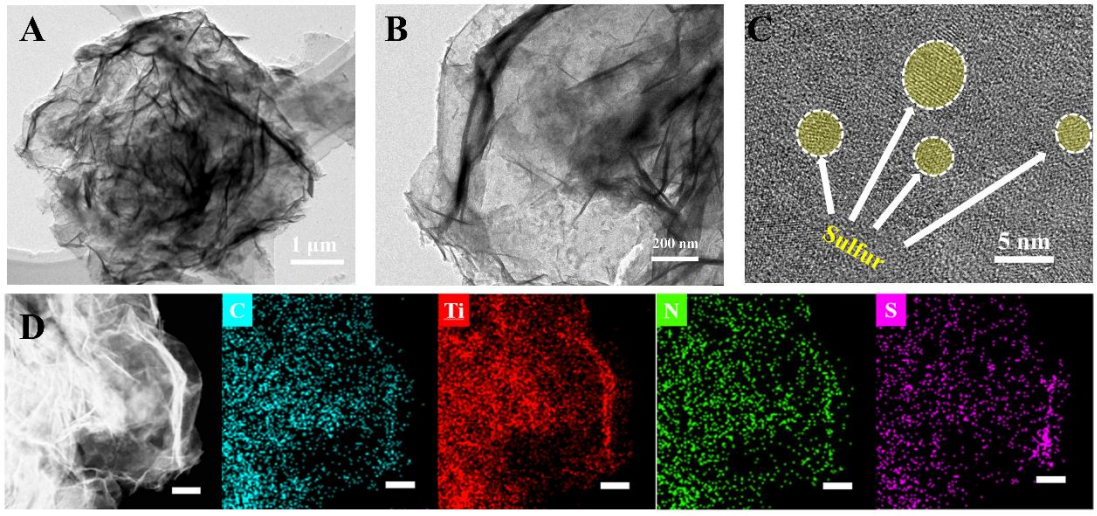

Supplementary Figure 4. (A, B) TEM, (C) HRTEM, and (D) STEM with corresponding elemental mappings of C, Ti, N, and S of 3D N-$Ti_3C_2T_x$/S. Scale bars:200 nm (D).

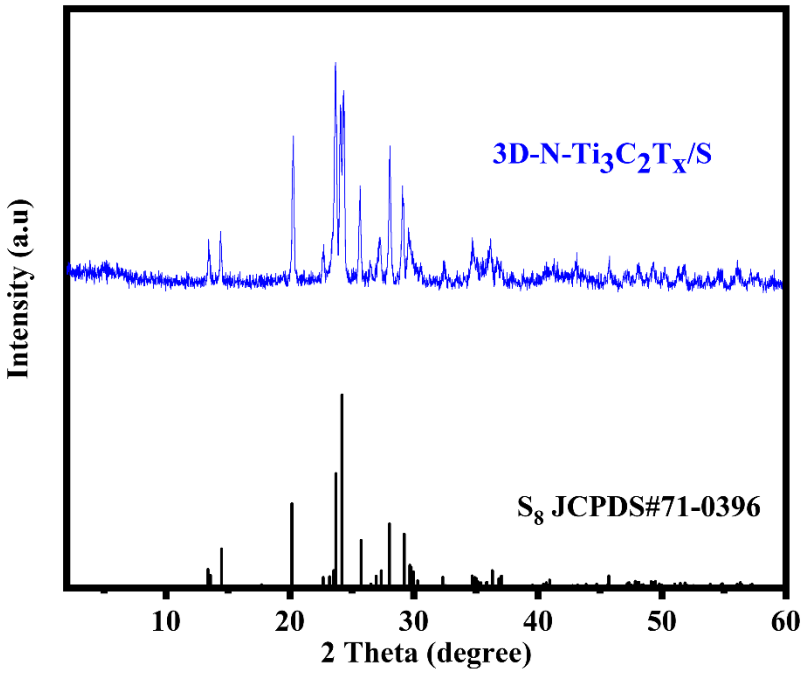

Supplementary Figure 5. XRD patterns of 3D N-$Ti_3C_2T_x$/S and S_8.

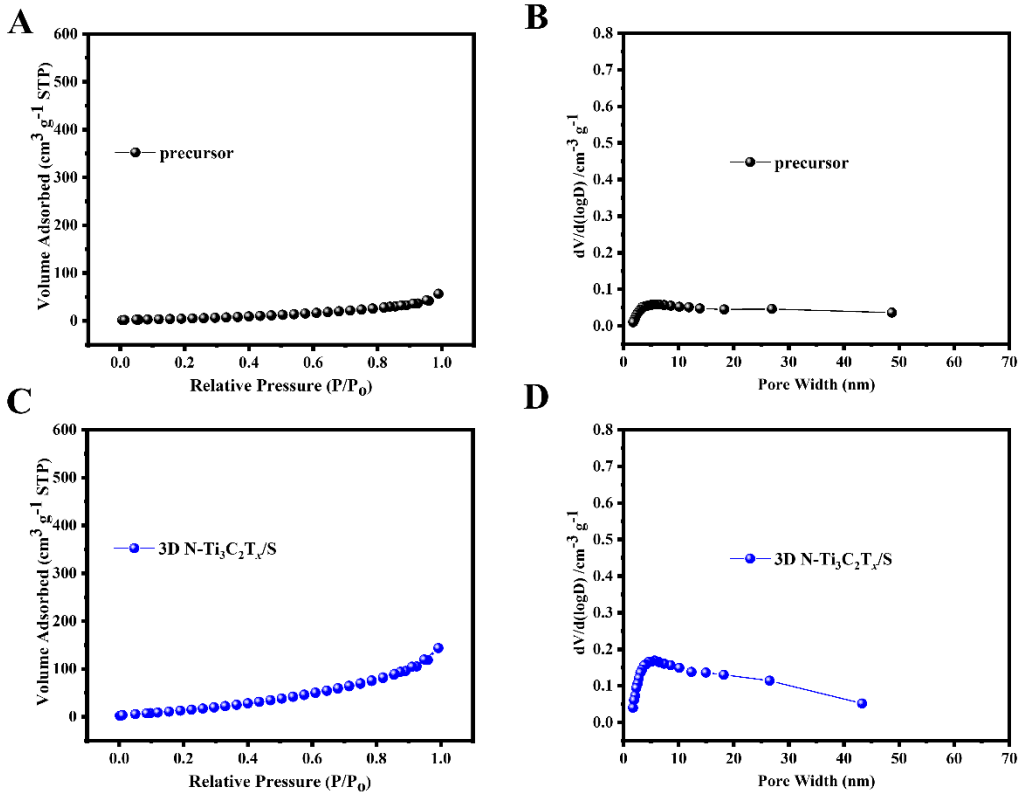

Supplementary Figure 6. (A, C) N_2 adsorption-desorption isotherms and (B, D) pore-size distribution curves of melamine/MXenes precursor and 3D N-$Ti_3C_2T_x$/S.

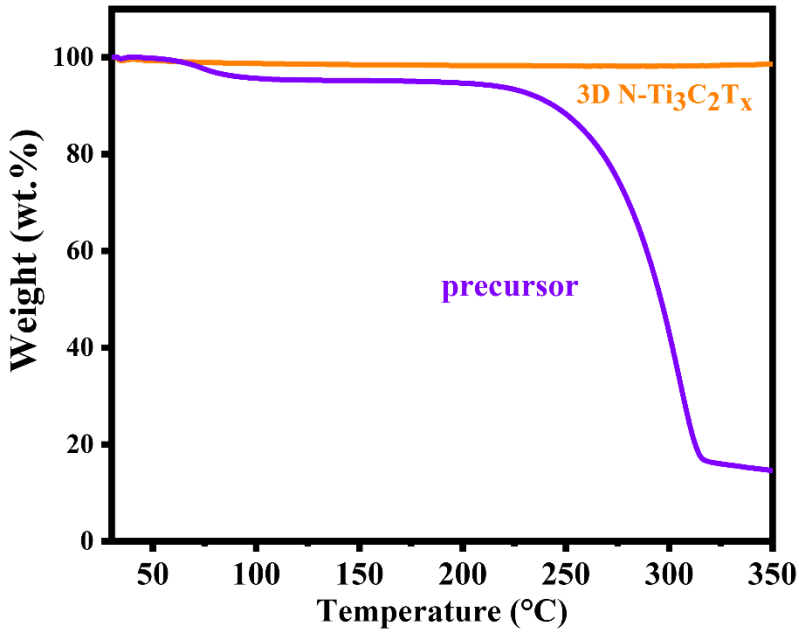

Supplementary Figure 7. TGA curves in Ar atmosphere of 3D N-$Ti_3C_2T_x$ and HCl-treated melamine/MXenes precursor.

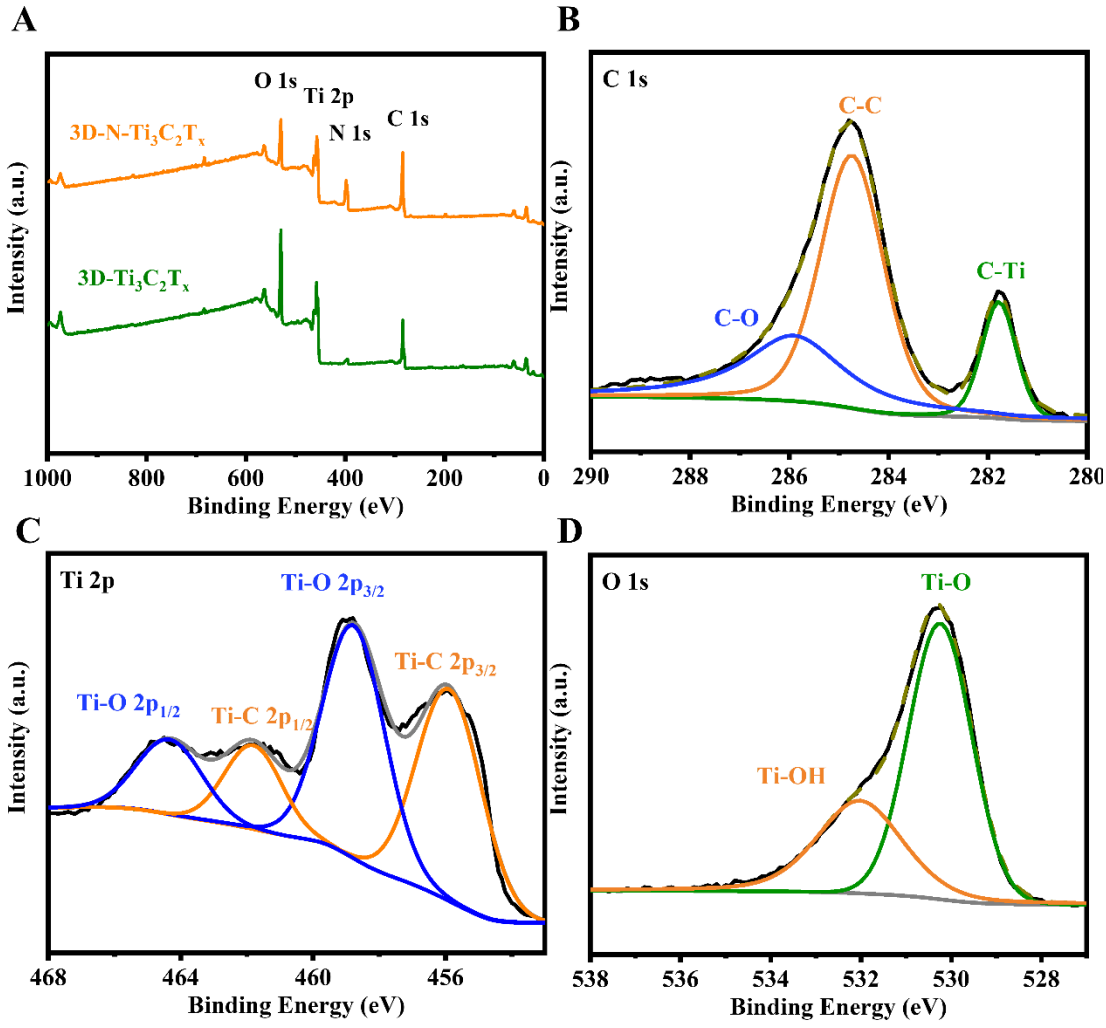

Supplementary Figure 8. (A) XPS spectrum of 3D N-$Ti_3C_2T_x$ and 3D $Ti_3C_2T_x$. (B) C 1s, (C) Ti 2p and (D) O 1s spectra of 3D N-$Ti_3C_2T_x$.

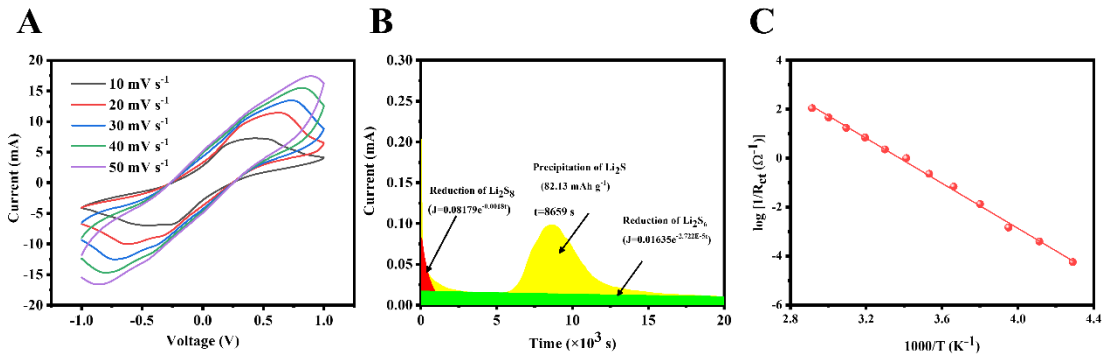

Supplementary Figure 9. (A) The CV curves of 3D $Ti_3C_2T_x$ symmetrical cell at the scan rate range from 10 mV s^{-1} to 50 mV s^{-1}. (B) The potentiostatic discharge profiles of Li_2S precipitation (at 2.05 V) for 3D $Ti_3C_2T_x$. (C) The Arrhenius plot of ionic conductivity obtained from R_{ct} collected in Fig. 4I versus temperature.

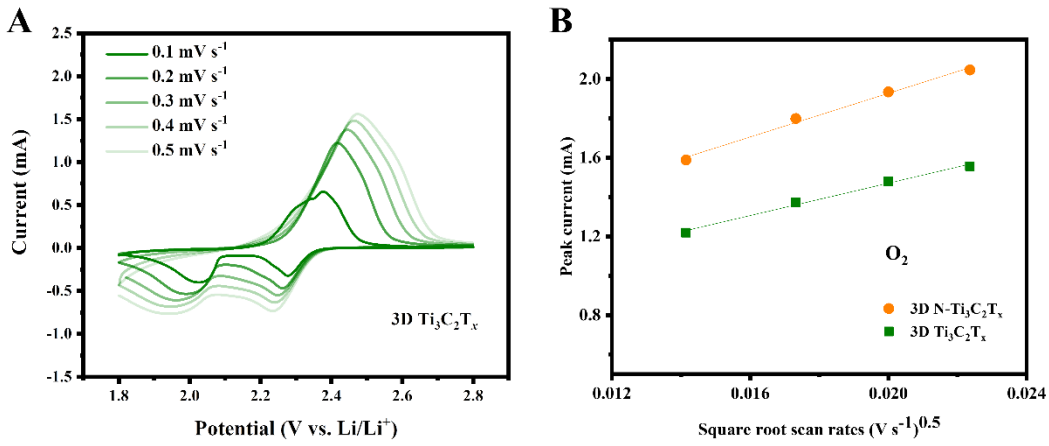

Supplementary Figure 10. (A) The CV curves of 3D $Ti_3C_2T_x$/S cathodes at different scan rates. (B) The plot of CV peak of O_2 (LiPSs-S_8) versus the square root of scan rates.

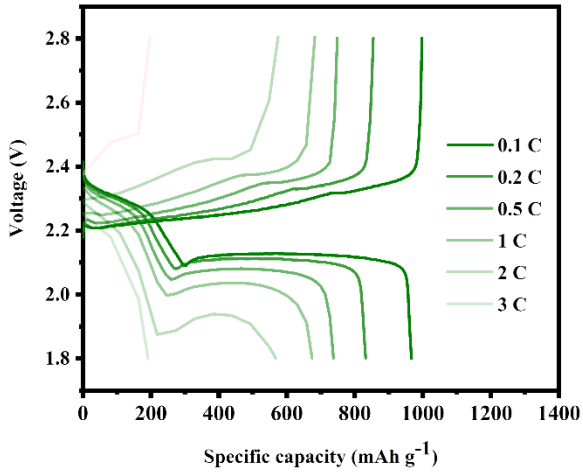

Supplementary Figure 11. The GCD profiles of 3D $Ti_3C_2T_x$/S at 0.1 C, 0.2 C, 0.5 C, 1 C, 2 C, and 3 C.

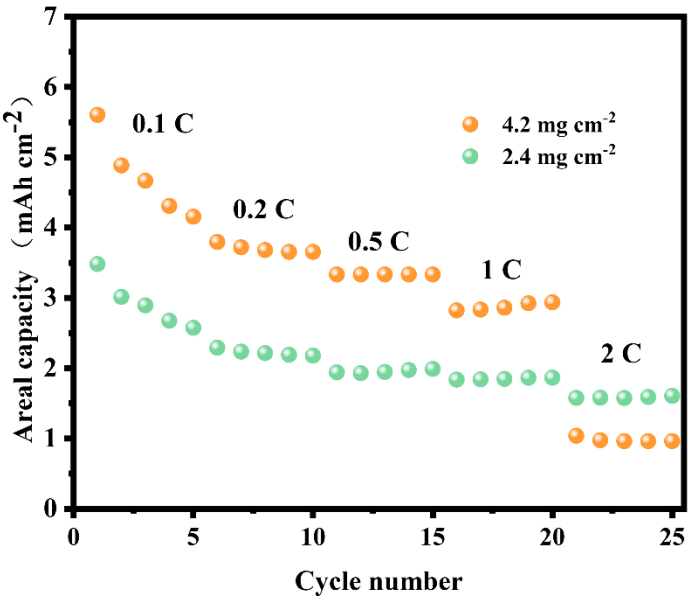

Supplementary Figure 12. The rate performance of the cells with high sulfur loading.

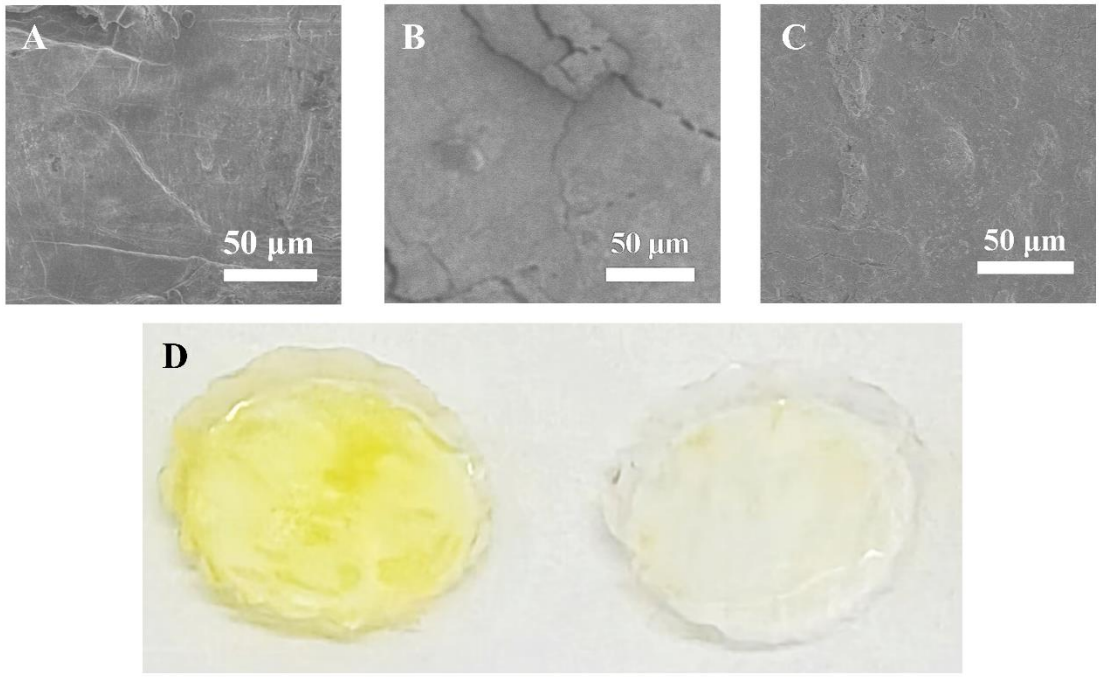

Supplementary Figure 13. (A) SEM image of the pristine lithium anode. SEM images of Li anodes paired with (B) 3D $Ti_3C_2T_x$/S and (C) 3D N-$Ti_3C_2T_x$/S cathodes after 100 cycles at 0.5 C. (D) Digital photo of cycled separators for N-$Ti_3C_2T_x$/S and 3D $Ti_3C_2T_x$/S cathodes.

Supplementary Table 1. The proportion of different configuration nitrogen before and after the adsorption of Li_2S_6.

	Pyrrolic N	Pyridinic N	Ti-N
Before adsorption	28.6%	41.9%	29.5%
After adsorption	44.4%	36.9%	18.7%